International Journal of Multiphase Flow 36 (2010) 882–890

Contents lists available at ScienceDirect

International Journal of Multiphase Flow

journal homepage: www.elsevier.com/locate/ijmulflow

Three-dimensional simulations of air–water bubbly flows

Xia Wang, Xiaodong Sun *

Nuclear Engineering Program, Department of Mechanical Engineering, The Ohio State University, 201 West 19th Avenue, Columbus, OH 43210, United States

ARTICLE INFO

Article history:
Received 5 April 2010
Received in revised form 6 August 2010
Accepted 6 August 2010
Available online 10 August 2010

Keywords:
Air–water bubbly flows
Interfacial area transport equation
Interfacial area concentration
Three-dimensional simulation
Lift force

ABSTRACT

Interfacial area transport equation (IATE) is considered promising to evaluate dynamic changes of the interfacial area concentration in gas–liquid two-phase flows, which is of significance in characterizing the interfacial structure of the flows. Efforts were made by the authors in the past on the implementation of the IATE into computational fluid dynamics codes, such as Fluent. However, it remained unclear whether the IATE model coefficients derived from one-dimensional IATE model calibrations can be applied to three-dimensional simulations. The current study aimed to examine, primarily by investigating the lateral profiles of phase distributions, the applicability of the coefficients obtained from the one-dimensional IATE model calibration to a three-dimensional simulation of bubbly flow in a pipe. In addition, effects of the lift force on the lateral phase distributions were studied. A new set of the IATE model coefficients was suggested for a three-dimensional bubbly flow simulation. Good agreement was obtained with the updated coefficients between the predicted and measured flow parameters.

1. Introduction

In the two-fluid model, knowledge of the interfaces that separate different phases in two-phase flows is a key to accurately predict gas–liquid two-phase flows. To characterize the interfacial structure, the interfacial area concentration (IAC), a geometric parameter defined as the total interfacial surface per unit mixture volume, is introduced (Ishii and Mishima, 1980). There are several ongoing studies to model the IAC, one of which is the development of the interfacial area transport equation (IATE). Pioneering work on the formulation of the IATE was performed by Kocamustafaogullari and Ishii (1995). It was emphasized that the IATE was capable of modelling changes in the two-phase flow structure dynamically and mechanistically since it takes into account the bubble coalescence and disintegration caused by fluid particle interactions as well as phase changes due to boiling, evaporation or condensation. In generalized gas–liquid two-phase flows, bubbles observed in different sizes and shapes behave differently in terms of relative motion and interaction mechanisms. In view of this, bubbles are categorized into various groups with its own transport phenomena analogous to the basic concept of multi-group neutron transport theory. For a special case of bubbly flows, all of the bubbles are in spherical or distorted shape and thus can be treated as one group; therefore, a one-group IATE was recommended and developed (Wu et al., 1998). It is also noteworthy that two-group IATE has been proposed to be applicable to a wide range of flow regimes beyond bubbly flows (Fu and Ishii, 2003a; Smith, 2002; Sun et al., 2004).

One of the challenges in establishing the IATE is to construct appropriate closure relations of bubble–bubble and bubble–eddy interactions. Previous studies show that for most bubbly flows there were three major mechanisms, namely, bubble disintegration caused by the impact of turbulence eddies (TI), bubble coalescence due to wake entrainment (WE), and bubble coalescence caused by turbulence-driven random collisions (RC). Theoretical model of each mechanism was derived with adjustable coefficients that varied with flow channel configuration (Kim, 1999; Ishii et al., 2002; Kim et al., 2003). Continuous efforts have been made to determine these coefficients by comparing numerical results to experimental measurements. Kim (1999) used the one-dimensional two-fluid model and a one-dimensional one-group IATE to calculate the phase distributions for flow in a narrow rectangular channel. During this calibration process, the values of the coefficients in the one-dimensional one-group IATE were suggested based on comparisons with experimental data. Similar work was carried out by Ishii et al. (2002) later for bubbly flows in different sizes of circular pipes. All of their work showed acceptable predictions of flow parameters along the flow direction.

Recently, capabilities of computational fluid dynamics (CFD) codes together with the IATE model for two-phase flow simulation have been examined. Graf and Papadimitriou (2007) demonstrated that the IAC could be reasonably captured by *FLU*BOX code equipped with the IATE in upward vertical pipe flows. Bae et al. (2008) developed a CFD code based on the finite volume method using the simplified marker and cell algorithm and coupled the two-fluid model and the one-group IATE systematically. Wang

* Corresponding author. Tel.: +1 6142477646.
E-mail addresses: wang.1037@osu.edu (X. Wang), sun.200@osu.edu (X. Sun).

0301-9322/$ - see front matter © 2010 Elsevier Ltd. All rights reserved.
doi:10.1016/j.ijmultiphaseflow.2010.08.004

and Sun (2007, 2009) implemented the one-group IATE into Fluent code and conducted three-dimensional simulations for bubbly flows in a rectangular duct and a round pipe. In addition, Sari et al. (2009) performed two- and three-dimensional simulations of isothermal bubbly flows by introducing the IATE model into the Fluent code. They pointed out that different researchers suggested different adjustable model coefficients for the same bubble interaction mechanism in the IATE model and showed differences between the predictions in the two- and three-dimensional simulations. Alongside with the IATE model, bubble number density (BND) transport equation was also developed to obtain the information on the changes of bubble number density. The BND model was successfully implemented into CFX (Cheung et al., 2007) for three-dimensional simulations. In all of these studies, the model coefficients in the IATE model that were determined based on one-dimensional calibrations were used for either two- or three-dimensional simulations. Nevertheless, the predictions of the lateral phase distributions presented in these studies were considerably improved compared to the numerical results without the IATE model even though there existed some discrepancies with experiments for some flow conditions. The above observation suggests that the disagreement could be caused by the use of the one-dimensional IATE model coefficients in the multi-dimensional simulations. Therefore, in this study, an attempt was made to address this issue.

The principal objectives of the present work are to investigate the contributions of non-uniform lateral phase distributions to the source/sink terms of the one-group IATE and to test the applicability of the coefficients derived by Ishii et al. (2002) to a three-dimensional simulation under pipe bubbly flow conditions. In addition, effects of the lift force on the lateral phase distributions are studied. Finally, a slightly different set of adjustable coefficients in the one-group IATE are suggested for three-dimensional simulations.

2. Implementation approach

Fluent, a control-volume-based code for multiple mesh styles, is chosen as the CFD tool for two-phase flows. In the conventional Fluent 6.3.33 code, however, the interactions among bubbles and between bubbles and turbulent eddies are not taken into account and bubble size must be specified by users (Fluent User's Guide, 2006). In order to capture the dynamic evolution of the interfacial structure, efforts have been made to implement the one-group IATE into Fluent (Wang and Sun, 2009). In what follows, the implementation approach is discussed briefly.

The one-group IATE for an isothermal adiabatic bubbly flow is given as (Wu et al., 1998)

$$\frac{\partial a_i}{\partial t}+\nabla\cdot(a_i\vec{v}_i)\cong\frac{2}{3}\left(\frac{a_i}{\alpha}\right)\left(\frac{\partial\alpha}{\partial t}+\nabla\cdot(\alpha\vec{v}_g)\right)+\frac{1}{3\psi}\left(\frac{\alpha}{a_i}\right)^2\sum_j R_j, \tag{1}$$

where a_i, $\vec{v}_i$, α, $\vec{v}_g$ and R_j are the interfacial area concentration, interfacial velocity, void fraction, gas velocity, and bubble number density change rate due to bubble interactions, respectively. If bubbles are well dispersed with spherical or close to spherical shape, the bubble shape factor ψ equals $1/(36\pi)$. In addition, $\vec{v}_i$ may be approximated as $\vec{v}_g$.

Despite the importance of the IAC, this parameter is not used in Fluent. Instead, the code uses the bubble diameter and void fraction information. In the current study, IAC is introduced as a user-defined scalar (UDS) in the gas phase domain, which is solved in Fluent based on the associated transport equation as

$$\frac{\partial(\alpha\rho_g a_i)}{\partial t}+\nabla\cdot(\alpha\rho_g\vec{v}_g a_i-\alpha\Gamma_g\nabla a_i)=S_g, \tag{2}$$

where ρ_g, Γ_g, and S_g denote the gas density, diffusion coefficient of the IAC, and source term, respectively. There is no physical diffusion of the IAC in the flow field, leading Γ_g in Eq. (2) to zero. S_g is determined by a comparison with Eq. (1) as

$$S_g=-(\alpha a_i\rho_g)\nabla\cdot\vec{v}_g+\frac{2a_i\rho_g}{3}\left[\frac{\partial\alpha}{\partial t}+\nabla\cdot(\alpha\vec{v}_g)\right]+\frac{\rho_g\alpha^3}{3\psi a_i^2}(R_{TI}+R_{WE}+R_{RC}). \tag{3}$$

Wu et al. (1998) identified three major interaction mechanisms in bubbly flows: bubble break-up due to the impact of turbulent eddies (R_{TI}), bubble coalescence caused by the wake entrainment (R_{WE}), and bubble coalescence due to the random collision driven by turbulence (R_{RC}). They were modelled by Wu et al. (1998) and Kim (1999) as

$$R_{TI}=\frac{C_{TI}\psi}{6}\left(\frac{a_i^4}{\alpha^3}\vec{v}_t\right)\sqrt{1-\frac{We_{cr}}{We}}\exp\left(-\frac{We_{cr}}{We}\right),\quad \text{if } We>We_{cr}, \tag{4}$$

$$R_{WE}=-36\psi^2C_{WE}C_D^{1/3}\frac{a_i^4\vec{v}_r}{\alpha^2}, \tag{5}$$

$$R_{RC}=-\frac{36\psi^2C_{RC}a_i^4\vec{v}_t}{\alpha^2\alpha_{\max}^{1/3}\left(\alpha_{\max}^{1/3}-\alpha^{1/3}\right)}\left[1-\exp\left(-\frac{C\alpha_{\max}^{1/3}\alpha^{1/3}}{\left(\alpha_{\max}^{1/3}-\alpha^{1/3}\right)}\right)\right]. \tag{6}$$

In Eq. (4), We is the Weber number, defined as the ratio of the bubble turbulent inertial energy to the surface energy as

$$We=\rho_f|\vec{v}_t|^2D_{avg}/\sigma, \tag{7}$$

where ρ_f, $\vec{v}_t$, D_{avg}, and σ are, respectively, the liquid density, turbulent velocity for the liquid phase, average diameter of bubbles, and surface tension between the two phases. The critical value, We_{cr}, is used to describe the balance state between the cohesive force due to surface tension and disruptive force by the turbulent eddies. In Eqs. (4)–(6), C_D, $\vec{v}_r$, and $\alpha_{\max}$ are the drag coefficient, relative velocity between the gas and liquid phases, and void fraction at the bubble maximum packing, respectively. Furthermore, C_{TI}, C_{WE}, C_{RC}, and C are the adjustable model coefficients, whose values were obtained earlier from several one-dimensional benchmarks based on an extensive database (Kim, 1999; Ishii et al., 2002; Kim et al., 2003). More details of the IATE implementation into Fluent are referred to Wang and Sun (2009).

3. Interfacial forces

The interfacial area concentration affects the flow field through the interfacial mass, momentum, and energy transfer. Assuming no mass exchange between the two phases for adiabatic flow, the ensemble-averaged momentum equation for the gas phase in the Eulerian multiphase model is written as (Fluent User's Guide, 2006)

$$\frac{\partial(\alpha\rho_g\vec{v}_g)}{\partial t}+\nabla\cdot\left(\alpha\rho_g\vec{v}_g\vec{v}_g\right)=-\alpha\nabla p+\nabla\cdot\bar{\bar{\tau}}_g+\alpha\rho_g\vec{g}+\vec{R}_{fg}+\vec{F}_g+\vec{F}_l+\vec{F}_{vm}, \tag{8}$$

where p, $\bar{\bar{\tau}}_g$, $\vec{g}$, $\vec{R}_{fg}$, $\vec{F}_g$, $\vec{F}_l$, and $\vec{F}_{vm}$ are the pressure, stress–strain tensor, gravitational acceleration, interaction force, additional external body force, lift force, and virtual mass force, respectively. The interaction force is comparable to the steady-state drag force, given by

$$\vec{R}_{fg}\approx-\frac{a_i}{8}C_D\rho_f\vec{v}_r|\vec{v}_r|\left(\frac{D_{sm}}{D_d}\right). \tag{9}$$

Here, D_{sm} is the bubble Sauter mean diameter defined as $D_{sm} = 6\alpha/a_i$ and D_d is bubble drag diameter. These two diameters are approximately the same in bubbly flows. For the drag coefficient C_D, the model suggested by Tomiyama (1998) for slightly-contaminated air–water two-phase flows is adopted in this study:

$$C_D = \max\left\{\min\left[\frac{24}{\mathrm{Re}_b}\left(1+0.15\mathrm{Re}_b^{0.687}\right), \frac{72}{\mathrm{Re}_b}\right], \frac{8Eo}{3(Eo+4)}\right\}, \tag{10}$$

where two dimensionless numbers, namely, Eotvos number (Eo) and bubble Reynolds number (Re_b) are defined as $Eo = \frac{g(\rho_f-\rho_g)D_d^2}{\sigma}$ and $\mathrm{Re}_b = \frac{\rho_f|\vec{v}_r|D_d}{\mu_f}$.

The shear-induced lift force is of importance to the lateral phase distribution and given as

$$\vec{F}_l = -C_l\alpha\rho_f\vec{v}_r\times(\nabla\times\vec{v}_f), \tag{11}$$

where C_l is the lift force coefficient. Tomiyama (1998) combined the shear lift force (Zun, 1980; Auton, 1987; Drew and Lahey, 1987) and effects from slanted wake, and proposed a lift force coefficient model as

$$C_l = \begin{cases} \min[0.288\tanh(0.121\mathrm{Re}_b), f(Eo_b)], & \text{if } Eo_b < 4 \\ f(Eo_b), & \text{if } 4 \leqslant Eo_b \leqslant 10 \\ -0.29, & \text{if } Eo_b > 10 \end{cases} \tag{12}$$

where $f(Eo_b) = 0.00105Eo_b^3 - 0.0159Eo_b^2 - 0.0204Eo_b + 0.474$. In Eq. (12), the modified Eotvos number, Eo_b, is defined based on the maximum horizontal dimension of a bubble, D_H, which is calculated as $D_H = D_d(1+0.163Eo^{0.757})^{1/3}$, to account for the influences from the deformation of bubbles.

Wall lubrication and turbulent dispersion forces are also considered in the current study. The former is due to the asymmetric drainage of the liquid around the rising bubble near a wall while the latter is driven by the void fraction gradient. Antal et al. (1991) deduced a two-dimensional analytical solution of the wall lubrication force based on the complex potential function of flows as

$$F_w = \frac{2\alpha\rho_f|\vec{v}_\parallel|^2}{D_d}\left[C_{w1}+C_{w2}\left(\frac{D_d}{2d_{bw}}\right)\right]\vec{n}_w, \tag{13}$$

with $\vec{v}_\parallel = \vec{v}_r - [\vec{n}_w\cdot\vec{v}_r]\vec{n}_w$, $C_{w1} = -0.104 - 0.06\vec{v}_r$, and $C_{w2} = 0.147$. Here, d_{bw} and $\vec{n}_w$ are respectively the distance between the bubble and the wall, and the unit outward normal vector to the wall surface. The turbulent dispersion force, analogous to the molecular dispersion force, tends to flatten the void fraction distribution. The constitutive equation of the turbulent dispersion force is given as (Lahey et al., 1993):

$$M_d^T = -C_T\rho_f k_f\nabla\alpha, \tag{14}$$

where k_f is the total turbulent kinetic energy of the liquid phase and coefficient C_T is taken as 0.1.

Any transient two-phase flow will also experience transient forces, such as the virtual mass force and Basset force (Drew and Lahey, 1987; Michaelides, 1997). They are important not only to provide accurate predictions of flow distributions, but also to stabilize the numerical solutions in general. Since the flow of interest in the current study is quasi-steady-state, the transient forces are neglected.

4. Turbulence model

The above discussion indicates that the bubble interaction models rely strongly on the turbulence. In addition, a mechanistic turbulence model is essential to provide closure for the Reynolds stress tensor in Eq. (8). In Eqs. (4) and (6), the magnitude of turbulent velocity, v_t, can be evaluated based on the Kolmogorov's universal equilibrium theory in the inertial sub-range of isotropic homogeneous turbulence as (Batchelor, 1951; Rotta, 1972):

$$v_t = 1.4\varepsilon_f^{1/3}D_d^{1/3}. \tag{15}$$

In this study, standard dispersed $k-\varepsilon$ turbulence model is selected, in which the transport equations of turbulent kinetic energy and turbulent dissipation rate for the liquid phase, i.e., k_f and ε_f, are given as

$$\begin{aligned}&\frac{\partial}{\partial t}[(1-\alpha)\rho_f k_f] + \nabla\cdot[(1-\alpha)\rho_f k_f\vec{v}_f] \\ &= \nabla\cdot\left[(1-\alpha)\left(\mu+\frac{\mu_f^t}{\sigma_k}\right)\nabla k_f\right] + (1-\alpha)P_f - (1-\alpha)\rho_f\varepsilon_f \\ &\quad + (1-\alpha)\Phi_k,\end{aligned} \tag{16}$$

$$\begin{aligned}&\frac{\partial}{\partial t}[(1-\alpha)\rho_f \varepsilon_f] + \nabla\cdot[(1-\alpha)\rho_f \varepsilon_f\vec{v}_f] \\ &= \nabla\cdot\left[(1-\alpha)\left(\mu+\frac{\mu_f^t}{\sigma_\varepsilon}\right)\nabla\varepsilon_f\right] + C_{\varepsilon 1}\frac{(1-\alpha)P_f\varepsilon_f}{k_f} - C_{\varepsilon 2} \\ &\quad \times\frac{(1-\alpha)\varepsilon_f^2}{k_f} + (1-\alpha)\Phi_\varepsilon,\end{aligned} \tag{17}$$

where P_f is the production of turbulence kinetic energy due to the mean velocity gradients. The turbulence influenced by the gas phase due to the bubbles agitation is taken into account by the source terms Φ_k and Φ_ε that are specified by users with the relation of

$$\Phi_k = \frac{k_f}{C_{\varepsilon 3}\varepsilon_f}\Phi_\varepsilon. \tag{18}$$

In our study, the constitutive relation of Φ_k is furnished by (Fluent User's Guide, 2006)

$$\Phi_k = \frac{3}{4D_d}\alpha\rho_f C_D|\vec{v}_r|\left[\frac{2k_f(b-1)}{1+\eta_{gl}} + \vec{v}_r\cdot\vec{v}_{dr}\right], \tag{19}$$

where $\vec{v}_{dr}$ is the drift velocity; the coefficient η_{gl} stands for the ratio of the bubble Lagrangian time scale to its characteristic relaxation time; and coefficient b is calculated as

$$b = (1+C_v)\left(\frac{\rho_g}{\rho_f}+C_v\right)^{-1}, \tag{20}$$

where C_v is the added mass coefficient. In addition, bubble-induced turbulence attributes to the two-phase turbulent viscosity, μ_f^t, which is customized based on Lahey's model (2005) as

$$\mu_f^t = C_\mu\frac{k_f^2}{\varepsilon_f} + 0.6D_{sm}\alpha|\vec{v}_r|. \tag{21}$$

The model constants are given as

$$C_{\varepsilon 1} = 1.44,\quad C_{\varepsilon 2} = 1.92,\quad C_{\varepsilon 3} = 1.2,\quad C_v = 0.5,$$
$$C_\mu = 0.09,\quad \sigma_k = 1.0,\quad \sigma_\varepsilon = 1.3.$$

The corresponding turbulent parameters for the gas phase are provided using Tchen-theory correlations based on the values of the liquid phase (Hinze, 1975). The so-called standard wall function bridges the near-wall region between the wall and turbulent core. More details can be found in Fluent User's Guide (2006).

5. Results and discussions

5.1. Flow conditions

Three-dimensional simulations were performed for a co-current upward air–water bubbly flow in a vertical pipe with an inner diameter of 48.3 mm (Fu, 2001). Table 1 summarizes the experimental conditions, including the superficial velocities of the gas and liquid phases, void fraction, IAC, and bubble Sauter mean diameter at the location of 5 pipe diameters away from the inlet, i.e., $z/D = 5$, where D is the inner diameter of the pipe. The superficial velocities of the gas and liquid phases range from 0.039 to 1.275 m/s, and 0.064 to 5.1 m/s, respectively. All of these flows fall into bubbly flow condition on a flow regime map (Mishima and Ishii, 1984) as shown in Fig. 1.

This argument being in bubbly flow is examined by considering two geometrical bubble scales that bound the limits of the diameter for small bubbles, i.e., the maximum spherical bubble limit (D_{ds}) and maximum distorted bubble limit ($D_{d,\max}$) defined as (Ishii and Zuber, 1979)

$$D_{ds} = 4\sqrt{\frac{2\sigma}{g\Delta\rho}}\left(\frac{\mu_f^2}{\sqrt{\rho_f^2\sigma^3/(g\Delta\rho)}}\right)^{1/6}, \tag{22}$$

$$D_{d,\max} = 4\sqrt{\frac{\sigma}{g\Delta\rho}}. \tag{23}$$

Bubbles are in perfect spherical shape without wobbling motion until their diameters exceed D_{ds}. Beyond this size, bubbles start to become distorted. Furthermore, bubbles will transition to cap, slug or churn-turbulent bubbles when the bubble diameter is larger than $D_{d,\max}$. Under the current air–water flow condition, D_{ds} and $D_{d,\max}$ are calculated approximately as 2 and 10.7 mm, respectively. It is evident from Table 1 that the bubble Sauter mean diameter is below $D_{d,\max}$. In addition, the bubble Sauter mean diameters for all the flow conditions but Runs 5 and 10 are near 2 to 3 mm. In the experiment performed by Fu (2001), the local flow data were acquired at three axial locations, i.e., $z/D = 5$, 30 and 55, using multi-sensor conductivity probes, which have a measurement uncertainty less than 10% for the void fraction and IAC (Kim, 1999).

5.2. Three-dimensional simulations with model coefficients from Ishii et al. (2002)

As pointed out earlier, in early efforts of determining the model coefficients for the one-group IATE, almost all the calibrations were performed based on a steady-state one-dimensional assumption. The following IATE model coefficients were suggested by Ishii et al. (2002) for a medium-sized pipe:

Table 1
Flow conditions at $z/D = 5$.

Run #	j_g (m s^{-1})	j_f (m s^{-1})	α (%)	a_i (m^{-1})	D_{sm} (mm)
2	0.039	0.682	2.21	58.0	2.3
3	0.136	0.682	9.37	180	3.1
4	0.138	2.336	3.74	94.8	2.4
5	0.506	2.336	12.8	171	4.5
6	0.538	5.10	5.75	193	1.8
7	1.234	5.10	11.7	260	2.7
10	1.275	2.607	25.7	166	9.3
14	0.039	0.064	11.8	295	2.4
16	0.039	0.20	7.03	188	2.2
17	0.133	0.20	25.0	559	2.7

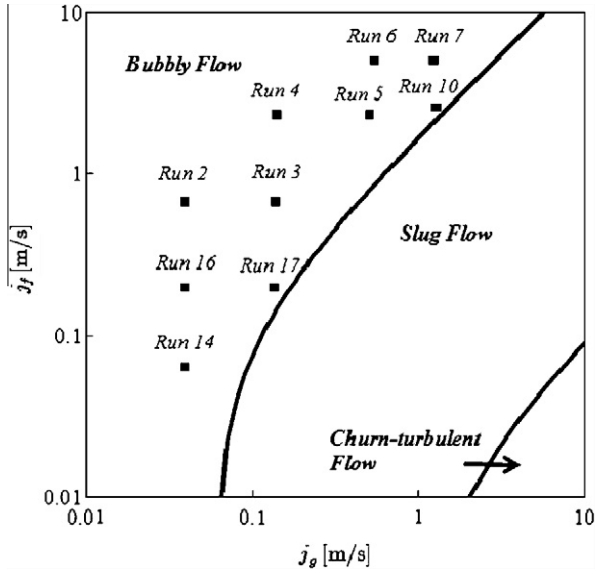

Fig. 1. Flow conditions in the flow regime map (Mishima and Ishii, 1984).

$$\begin{aligned}&\text{Turbulent impact}: C_{TI} = 0.0085; \quad We_{cr} = 6.0;\\ &\text{Wake entrainment}: C_{WE} = 0.002;\\ &\text{Random collision}: \ C_{RC} = 0.004; C = 3.0; \ \alpha_{\max} = 0.75.\end{aligned} \tag{24}$$

Their consistency and universal applicability have been validated by several studies, including the one by Fu and Ishii (2003b).

In the current study, three-dimensional numerical studies were first performed with the hypothesis that the coefficients from the one-dimensional model benchmark would be applicable to three-dimensional simulations. After a careful mesh sensitivity study, it was found that for the pipe test section, 380,160 cells with 900 nodes along the pipe axial direction are sufficient. A similar mesh sensitivity study can be found in Wang and Sun (2009). Profiles of the void fraction, IAC, and bubble velocity measured at $z/D = 5$ by Fu (2001) were applied as inlet boundary conditions. These profiles are non-uniform in the radial direction. Differences of the area-averaged IAC predictions ($\langle a_i^{num}\rangle$) and the area-averaged measurements ($\langle a_i^{exp}\rangle$) are quantified using the relative error, which is defined as

$$Error = \frac{\langle a_i^{num}\rangle - \langle a_i^{exp}\rangle}{\langle a_i^{exp}\rangle} \times 100[\%]. \tag{25}$$

As shown in Fig. 2, the relative errors at the locations of $z/D = 30$ and 55 are over 50% for the four experimental runs shown. The IAC is always overestimated in the simulation for these flow conditions, which implies that the break-up source term in the one-group IATE is over-predicted.

5.3. Discussions on the three-dimensional simulation

There are two possible issues existing in the one-dimensional IATE model when used for three-dimensional analysis. The first issue comes from the averaging process to obtain the one-dimensional IATE model from the three-dimensional model. In the averaging process, the covariance term representing the difference between the average of the product of two variables and the product of two averaged variables is ignored, i.e., $COV\langle AB\rangle = \langle AB\rangle - \langle A\rangle\langle B\rangle = 0$ (Kim, 1999). The other issue is related to the source term of the one-group IATE in Eq. (3), which includes the velocity divergence in the form of $-(a_i\alpha\rho_g)\nabla\cdot\vec{v}_g$. It is treated as $-a_i\alpha\rho_g\frac{\partial v_{gz}}{\partial z}$ in the one-dimensional form while it should be

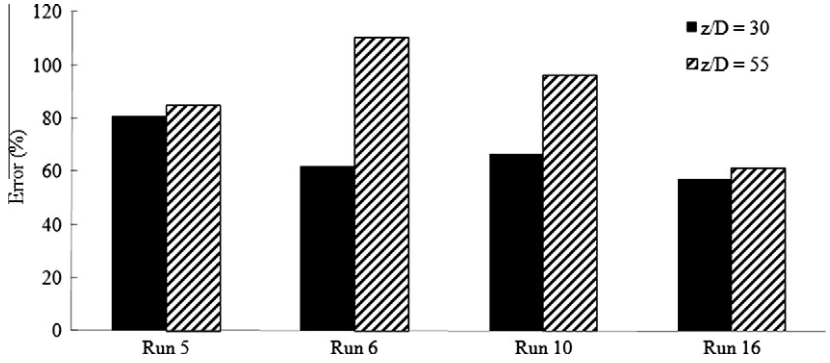

Fig. 2. Relative error of the IAC using model coefficients from Ishii et al. (2002).

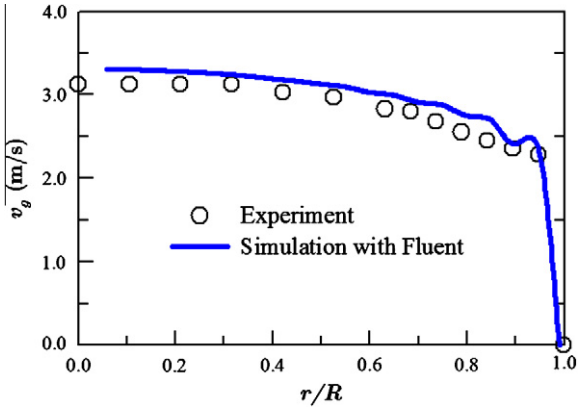

Fig. 3. Bubble velocity profile from experiment and simulation for Run 5.

$-a_i\alpha\rho_g(\frac{\partial v_{gx}}{\partial x}+\frac{\partial v_{gy}}{\partial y}+\frac{\partial v_{gz}}{\partial z})$ in a three-dimensional model. It is clearly seen that the additional contribution, i.e., from $\left(\frac{\partial v_{gx}}{\partial x}+\frac{\partial v_{gy}}{\partial y}\right)$, is omitted in the one-dimensional model. The above two issues would disappear if the lateral flow distributions are uniform, which however is not true for the current flow conditions. Fig. 3 shows the velocity profile across the cross section of the test section in Run 5. The predicted profile is in fairly satisfactory agreement with the measurement and apparently not uniform. The velocity gradient effect is especially important for the flow very near the wall. As a result, the model coefficients from Ishii et al. (2002) become inappropriate for three-dimensional simulations.

5.4. Testing of model coefficients in one-dimensional simulation

A study was carried out to examine the model coefficients that were obtained by Ishii et al. (2002) through a quasi-one-dimensional simulation. A three-dimensional simulation of Run 10 was constructed in a way where only the velocity gradient in z-direction (axial direction) was included for the term of $-(a_i\alpha\rho_g)\nabla\cdot\vec{v}_g$ in Eq. (3). Fig. 4a clearly shows that the predicted IAC along the radial direction at the elevation of $z/D = 55$ is in good agreement with the experimental data. The predicted void fractions at $z/D = 55$ from Fluent code with and without IATE are plotted with a comparison to the experimental data in Fig. 4b. The core peak observed in the experiment is captured if the one-group IATE was incorporated, which was illustrated more clearly in Fig. 4c by the contour plot of the void fraction from Fluent with the one-group IATE. This exercise basically demonstrated that the IATE model coefficients from Ishii et al. (2002) work reasonably in a simulation, where the radial velocity profile is considered uniform, i.e., quasi one-dimensional flow. However, the three-dimensional simulation for Run 10 using the same set of coefficients led to large errors as shown in Fig. 2.

5.5. Suggestions on model coefficients for three-dimensional IATE model

The exercise in Section 5.4 indicates that it is indispensable to develop appropriate coefficients in Eqs. (4)–(6) for a three-dimensional IATE model. The methodology of determining these coefficients is based on the experimental observations that the different bubble interaction mechanisms are predominant in different flow conditions. The coefficient for one bubble interaction term is possible to be estimated quasi-independently if for certain flow conditions, this term is significant and all other bubble interactions are either known or negligible. For instance, for flows with low flow rate, the dominant bubble interaction phenomenon is the wake entrainment, in which following bubbles inside the wake region of a preceding bubble catch up and collide with the preceding bubble. When the superficial liquid velocity becomes larger, an additional mechanism that would appear first is the random collision due to the higher turbulent intensity. When the superficial liquid velocity continues to increase such that the inertia of a turbulent eddy overcomes the surface tension force at a bubble interface, the bubble break-up phenomenon due to the turbulent impact starts to take place.

Assuming We_{cr}, C, and α_{max} remain the same as the values suggested by Ishii et al. (2002), the process of identifying the other model coefficients is illustrated as follows:

1. Determine C_{WE} when j_g and j_f are low;
2. Determine C_{RC} when j_g is high and j_f is still low. Here, C_{WE} is predetermined in step 1;
3. Determine C_{TI} when j_g and j_f are high. Here, C_{WE} and C_{WE} are determined in the previous two steps;
4. Check these adjustment coefficients for all flow conditions;
5. Adjust them iteratively until the relative errors between predictions and experimental data approach their minimum.

As a result, the following model coefficients yield the best fit to the experimental data in our three-dimensional simulations. The relative errors between the numerical and experimental results of the area-averaged IAC are within 15%, as shown in Fig. 5.

$$\begin{aligned}&\text{Turbulent impact}: C_{TI}=0.005,\ We_{cr}=6.0;\\ &\text{Wake entrainment}: C_{WE}=0.006;\\ &\text{Random collision}: C_{RC}=0.013,\ C=3.0,\alpha_{max}=0.75.\end{aligned}\tag{26}$$

In addition, the predicted IAC values using different coefficients at the location $z/D = 55$ are compared to the experimental data in Fig. 6 for Run 5. It is clearly seen that the IAC values using the

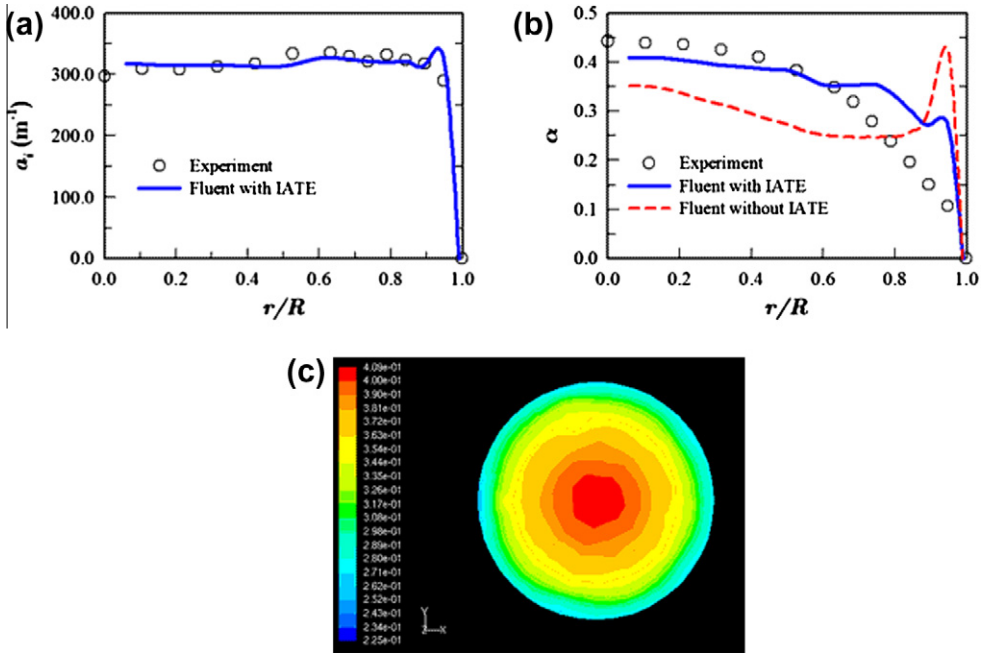

Fig. 4. Lateral distributions of Run 10 from simulations and experiments at the location $z/D = 55$: (a) the IAC, (b) the void fraction, and (c) counter of the void fraction from Fluent code with IATE.

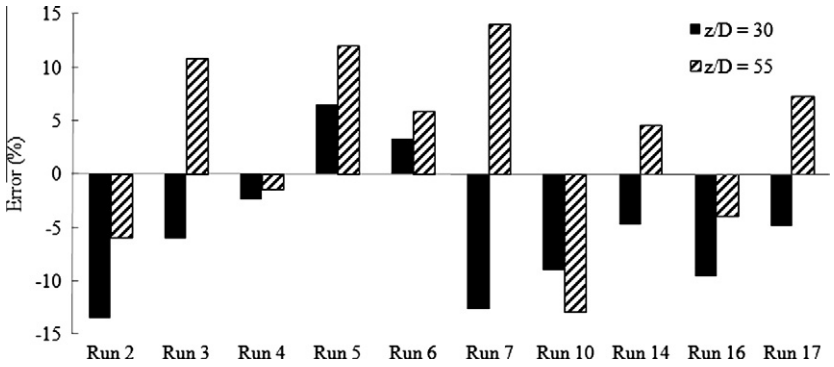

Fig. 5. Relative errors of IAC using the suggested model coefficients in Eq. (26).

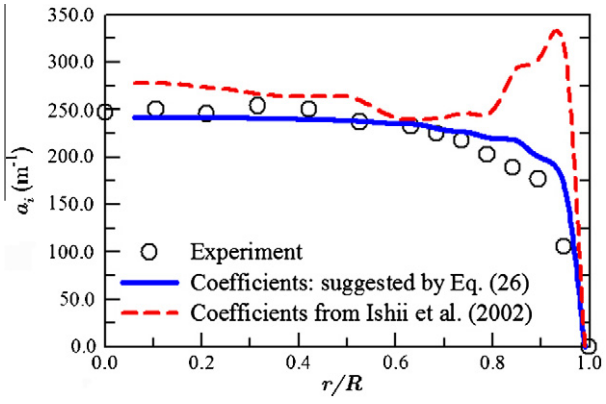

Fig. 6. Comparisons of IAC using different coefficients with experiments at the location $z/D = 55$ for Run 5.

coefficients suggested by Ishii et al. (2002) are overestimated, especially near the wall region. A distinct wall peak of IAC arises due to the contributions of the sharp velocity decrease close to the wall.

5.6. Study on the lift force

The shear-induced lift force, proportional to the vorticity of the liquid phase, is important for phase distributions in two-phase flows. The study on the lift force was performed with three different models available in Fluent: (1) Model 1: simulation without IATE and without lift force ($C_l = 0$); (2) Model 2: simulation without IATE and with a constant lift force coefficient; and (3) Model 3: simulation with IATE and with the lift force coefficient given by Eq. (12). Fig. 7 shows the void fraction with the three aforementioned models as compared to the experimental data acquired by Fu (2001) at $z/D = 55$ in Runs 2 and 5. In the conventional Fluent code without the IATE, the bubble size is considered to be constant, which is defined initially at the inlet. The lift force coefficient therefore can be determined based on the initial bubble size using Tomiyama's model given by Eq. (12), and it results in a value of about 0.25 for Model 2 in Runs 2 and 5. As we compare the predictions between Models 1 and 2 (the lift force coefficient was changed from 0 to 0.25), Model 2 provides a higher void fraction in the wall region (local wall peak), which indicates that the lift force pushes the small bubble towards the wall. In the Fluent simulation

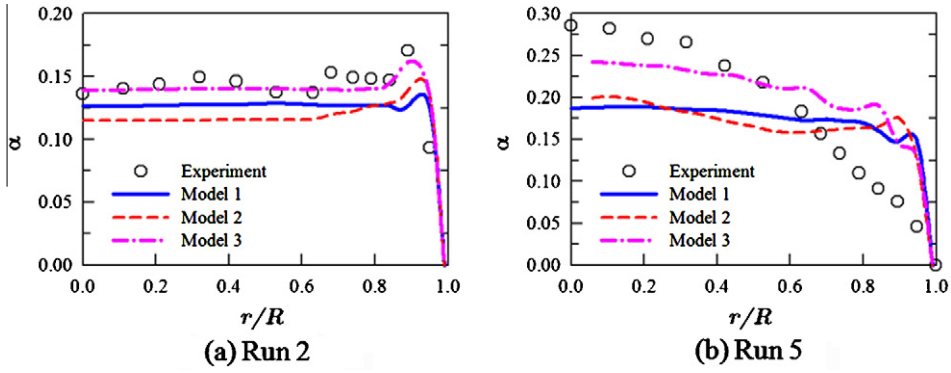

Fig. 7. Predictions of the void fraction with comparison to experiments at $z/D = 55$ for: (a) Run 2 and (b) Run 5.

with the IATE implemented (Model 3), the lift force coefficient is a function of bubble size and changes as the flow develops. It can be clearly seen that Model 3 provides closer agreement with experimental data for both flow conditions.

5.7. Results with three-dimensional simulations

Three-dimensional simulations were performed for all the flow conditions with the coefficients suggested by Eq. (26) in Section 5.5,

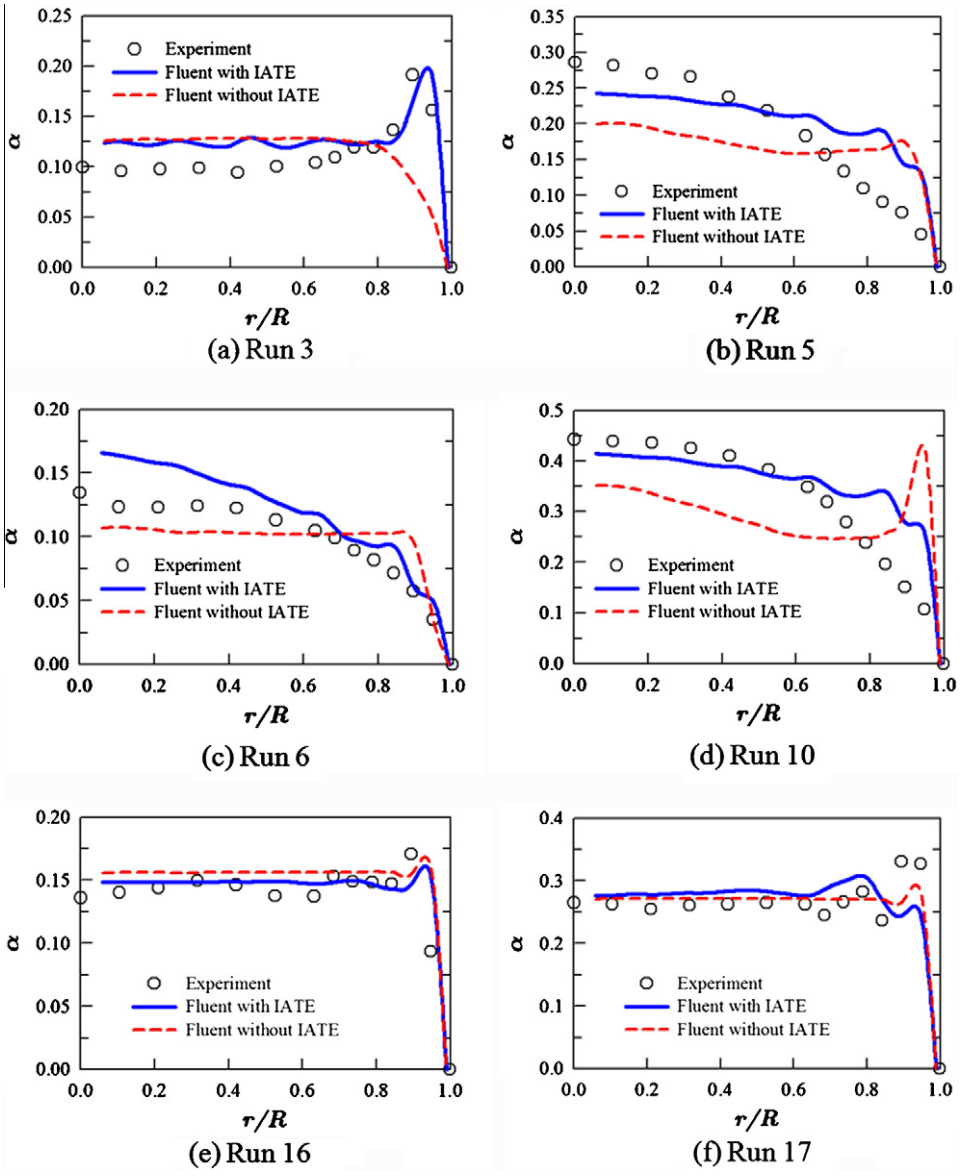

Fig. 8. Predictions of the void fraction with comparison to the experimental data at $z/D = 55$ for: (a) Run 3, (b) Run 5, (c) Run 6, (d) Run 10, (e) Run 16, and (f) Run 17.

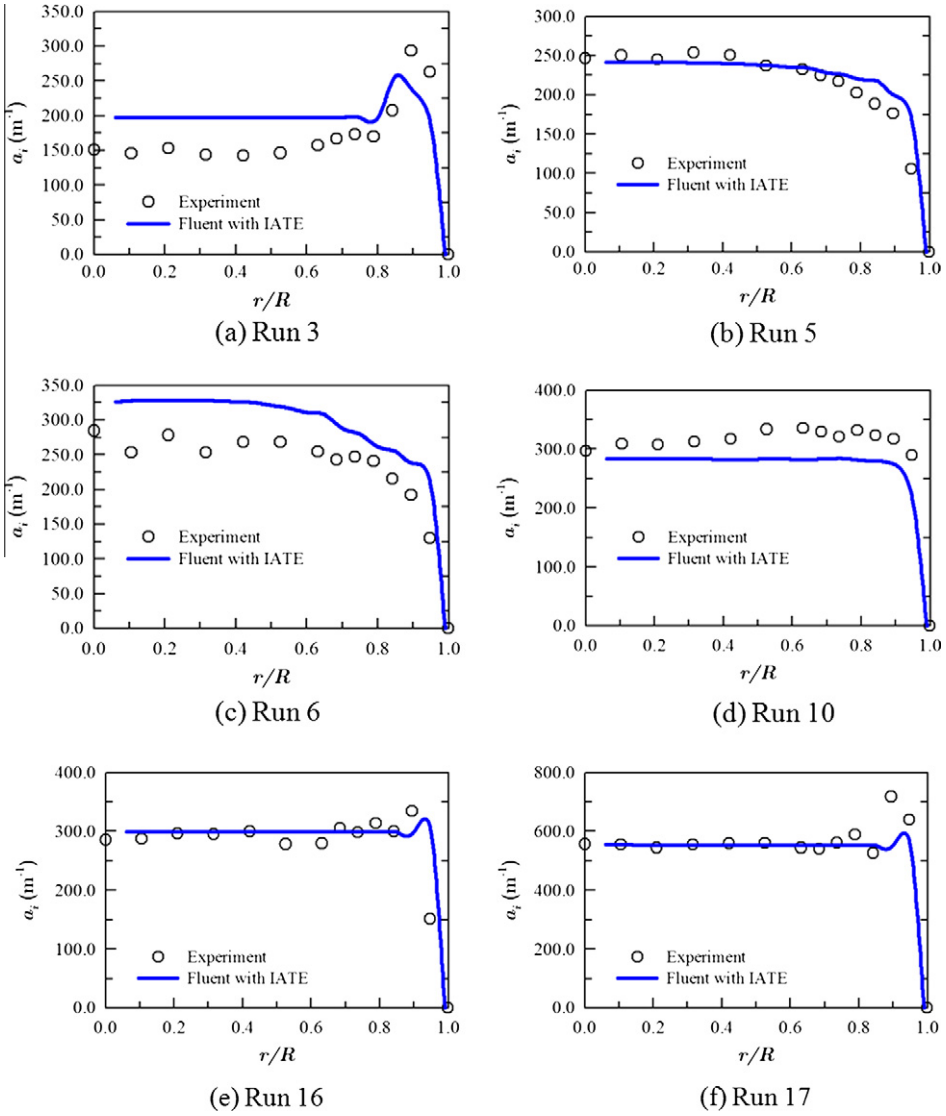

Fig. 9. Predictions of IAC with comparison to the experimental data at $z/D = 55$ for: (a) Run 3, (b) Run 5, (c) Run 6, (d) Run 10, (e) Run 16, and (f) Run 17.

and the simulation results are reported in Figs. 8 and 9. As shown in Fig. 8, the implementation of the one-group IATE considerably improves the predictive capability of the conventional Fluent code in terms of the phase distribution except for Runs 16 and 17. Run 16 has low superficial velocities and low void fraction. It was observed that in this run the axial pressure drop was a major contributor to the change of the void fraction along the flow direction. The bubble size in Run 16 was very close to D_{ds} and therefore bubbles did not actively interact with others in the neighborhood, i.e., bubble interactions became negligible. The distributions of the void fraction along the radial direction were almost flat except near the wall region, where a small peak appeared. This phenomenon could be captured by the Fluent code no matter whether the one-group IATE was applied. In Run 17, turbulent eddy impact was not strong enough to break up bubbles due to the relative low superficial velocity of the liquid phase. In contrast, bubble coalescence took place induced by both the random collision and wake entrainment, producing relatively larger bubbles such as cap and slug bubbles. It makes Run 17 close to the transition region, where the bubble transport mechanisms are further complicated (Sun et al., 2004). Therefore, the one-group IATE is not capable of describing these additional bubble interactions, requiring the application of a two-group IATE for Run 17.

As the IAC variable was introduced in Fluent, the predictions of IAC were plotted in Fig. 9 to help understand bubble interaction mechanisms and validate the models. Predictions of the IAC from the Fluent code with IATE match the experimental results qualitatively and quantitatively. For instance, it can be seen clearly that the peak of the IAC in the wall region in Run 3 is captured by both the experiment and simulation. A core peak of the IAC is observed in Runs 5 and 6 while a relatively flat profile of IAC is shown in other runs. A sharp decrease close to the wall occurs in all runs since the value of IAC on the wall is forced to zero.

6. Conclusion

In conclusion, the motivation of the present work is to obtain reliable predictions of air–water bubbly flows employing a CFD code Fluent with the implementation of the one-group IATE. This work indicates that the model coefficients in the one-group IATE obtained by Ishii et al. (2002) from a one-dimensional model calibration need to be re-calibrated for three-dimensional simulations of bubbly flow. The three-dimensional simulations with the new model coefficients show good agreement between numerical results and experimental data. It demonstrates remarkable advances

in the simulation of a dispersed two-phase flow system with the help of the one-group IATE model. In addition, effects of the lift force on the lateral phase distribution in bubbly flows are also discussed.

The one-group IATE is limited to bubbly flows only. Larger bubbles will be encountered in flow regime transition region and have substantial differences in their transport mechanisms from small bubbles. This requires the application of a two-group IATE. Though some deviations are found in the simulation from the experimental data, it is believed that the accuracy of Fluent code can be enhanced with the incorporation of the IATE model in the simulations of bubbly flow conditions.

Acknowledgments

Part of the work presented in this paper has been supported by a Junior Faculty Development Grant from the US Nuclear Regulatory Commission (Award No.: NRC-38-08-945). The authors would also like to acknowledge the computing resources and support provided by the Ohio Supercomputer Center. Comments related to the experimental data provided by Dr. M. Ishii of Purdue University and Dr. X. Fu of Applied Materials Inc., are appreciated.

References

Antal, S.P., Lahey, R.T., Flaherty, J.E., 1991. Analysis of phase distribution in fully developed laminar bubbly two-phase flow. Int. J. Multiphase Flow 17 (5), 635–652.

Auton, T.R., 1987. The lift force on a spherical body in a rotational flow. J. Fluid Mech. 183, 199–218.

Bae, B.U., Yoon, H.Y., Euh, D.J., Huh, B.G., Song, C.H., Park, G.C., 2008. Development of a multi-dimensional fluid dynamics code and its benchmarking for the subcooled boiling flow. Heat Transfer Eng. 29 (8), 667–676.

Batchelor, B.K., 1951. Pressure fluctuation in isotropic turbulence. Proc. Cambridge Philos. Soc. 47, 359–374.

Cheung, S.C.P., Yeoh, G.H., Tu, J.Y., 2007. On the numerical study of isothermal vertical bubbly flow using two population balance approaches. Chem. Eng. Sci. 62 (17), 4659–4674.

Drew, D.A., Lahey, R.T., 1987. The virtual mass and lift force on a sphere in rotating and straining inviscid flow. Int. J. Multiphase Flow 13 (1), 113–121.

Fluent User's Guide, 2006. Fluent Inc., Lebannon, USA.

Fu, X., 2001. Interfacial Area Measurement and Transport Modeling in Air–water Two-phase Flow. Ph.D. Thesis, School of Nuclear Engineering, Purdue University, West Lafayette, IN.

Fu, X., Ishii, M., 2003a. Two-group interfacial area transport in vertical air–water flow. I. Mechanistic model. Nucl. Eng. Des. 219 (2), 143–168.

Fu, X., Ishii, M., 2003b. Two-group interfacial area transport in vertical air–water flow. II. Model evaluation. Nucl. Eng. Des. 219 (2), 169–190.

Graf, U., Papadimitriou, P., 2007. Simulation of two-phase flows in vertical tubes with the CTFD code *FLU* BOX. Nucl. Eng. Des. 237, 2120–2125.

Hinze, J.O., 1975. Turbulence. McGraw-Hill, New York.

Ishii, M., Kim, S., Uhle, J., 2002. Interfacial area transport equation: model development and benchmark experiments. Int. J. Heat Mass Transfer 45 (15), 3111–3123.

Ishii, M., Mishima, K., 1980. Study of Two-fluid Model and Interfacial Area. ANL-80-111.

Ishii, M., Zuber, N., 1979. Drag coefficient and relative velocity in bubbly, droplet or particulate flows. AIChE J. 25 (5), 843–855.

Kim, S., 1999. Interfacial Area Transport Equation and Measurement of Local Interfacial Characteristics. Ph.D. Thesis, School of Nuclear Engineering, Purdue University, West Lafayette, IN.

Kim, S., Sun, X., Ishii, M., Beus, S.G., Lincoln, F., 2003. Interfacial area transport and evaluation of source and sink terms for confined air–water bubbly flow. Nucl. Eng. Des. 219, 61–75.

Kocamustafaogullari, G., Ishii, M., 1995. Foundation of the interfacial area transport equation and its closure relations. Int. J. Heat Mass Transfer 38 (3), 481–493.

Lahey, R.T., 2005. The simulation of multidimensional multiphase flows. Nucl. Eng. Des. 235 (10–12), 1043–1060.

Lahey, R.T., Debertodano, M.L., Jones, O.C., 1993. Phase distribution in complex geometry conduits. Nucl. Eng. Des. 141 (1–2), 177–201.

Michaelides, E.E., 1997. Review – the transient equation of motion for particles, bubbles, and drops. J. Fluid Eng. 119 (2), 233–247.

Mishima, K., Ishii, M., 1984. Flow regime transition criteria for upward two-phase flow in vertical tubes. Int. J. Heat Mass Transfer 27 (5), 723–737.

Rotta, J.C., 1972. Tubulente Stromungen. B.G. Teubner, Stuttgart.

Sari, S., Ergun, S., Barik, M., Kocar, C., Sokmen, C.N., 2009. Modeling of isothermal bubbly flow with interfacial area transport equation and bubble number density approach. Ann. Nucl. Energy 36 (2), 222–232.

Smith, T.R., 2002. Two-group Interfacial Area Transport Equation in Larger Diameter Pipes. Ph.D. Thesis, School of Nuclear Engineering, Purdue University, West Lafayette, IN.

Sun, X., Kim, S., Ishii, M., Beus, S.G., 2004. Modeling of bubble coalescence and disintegration in confined upward two-phase flow. Nucl. Eng. Des. 230 (1–3), 3–26.

Tomiyama, A., 1998. Struggle with computational bubble dynamics. In: Proceedings of the 3rd International Conference on Multiphase Flow (ICMF-1998), Lyon, France.

Wang, X., Sun, X., 2007. CFD simulation of phase distribution in adiabatic upward bubbly flows using interfacial area transport equation. In: Proceedings of the 12th International Topical Meeting on Nuclear Reactor Thermal Hydraulics (NURETH-12), Pittsburgh, PA.

Wang, X., Sun, X., 2009. CFD simulation of phase distribution in adiabatic upward bubbly flows using interfacial area transport equation. Nucl. Technol. 167 (1), 71–82.

Wu, Q., Kim, S., Ishii, M., Beus, S.G., 1998. One-group interfacial area transport in vertical bubbly flow. Int. J. Heat Mass Transfer 41 (8–9), 1103–1112.

Zun, I., 1980. The transverse migration of bubbles influenced by walls in vertical bubbly flow. Int. J. Multiphase Flow 6 (6), 583–588.